Vibrational anharmonicity and multilevel vibrational dephasing from vibrational echo beats

K. D. Rector, A. S. Kwok,[a] C. Ferrante,[b] and A. Tokmakoff[c]
Department of Chemistry, Stanford University, Stanford, California 94305

C. W. Rella
Hansen Experimental Physics Laboratory, Stanford University, Stanford, California 94305

M. D. Fayer[d]
Department of Chemistry, Stanford University, Stanford, California 94305

(Received 22 January 1997; accepted 21 March 1997)

Vibrational echo experiments were performed on the IR active CO stretching modes ($\sim 2000\ \mathrm{cm}^{-1}$) of rhodium dicarbonylacetylacetonate [$Rh(CO)_2acac$] and tungsten hexacarbonyl [$W(CO)_6$] in dibutylphthalate and a mutant of myoglobin-CO (H64V-CO) in glycerol–water using ps IR pulses from a free electron laser. The echo decays display pronounced beats and are nonexponential. The beats and nonexponential decays arise because the bandwidths of the laser pulses exceed the vibrational anharmonicities, leading to the excitation and dephasing of a multilevel coherence. From the beat frequencies, the anharmonicities are determined to be 14.7, 13.5, and 25.4 cm^{-1}, for $W(CO)_6$, $Rh(CO)_2acac$, and H64V-CO, respectively. From the components of the nonexponential decays, the vibrational dephasing at very low temperature of both the $v=0-1$ and $v=1-2$ transitions are determined. At the lowest temperatures, $T_2 \approx 2T_1$, so the $v=2$ lifetimes are obtained for the three molecules. These are found to be significantly shorter than the $v=1$ lifetimes. Although the $v=1$ lifetimes are similar for the three molecules, there is a wide variation in the $v=2$ lifetimes. © *1997 American Institute of Physics.* [S0021-9606(97)02324-6]

I. INTRODUCTION

The measurement of vibrational spectra using Fourier transform infrared (FTIR) spectroscopy provides a wealth of information about the equilibrium structures of molecules and the effects of solvents on normal modes. However, important types of measurements, i.e., vibrational homogeneous linewidth and the vibrational anharmonicity, are either difficult or impossible to perform with ordinary linear techniques. Measurements of vibrational anharmonicities provide information about the shape of the vibrational potential surface. Vibrational anharmonicities are not readily obtained using a conventional FTIR because the $v=0\rightarrow 2$ transition is forbidden, and, therefore, the absorption at the frequency corresponding to the $v=0\rightarrow 2$ transition is weak. In addition, the spectral region around a $v=0\rightarrow 2$ transition is frequently congested with combination bands, making it difficult to identify the correct peak. A direct measurement of the $v=1\rightarrow 2$ transition is not usually feasible for the higher frequency modes ($1000-4000\ \mathrm{cm}^{-1}$) because the thermal population at ambient temperatures of the $v=1$ state is down five to twenty factors of e compared to the $v=0$ state.

Another technique for measuring vibrational anharmonicity involves the use of time resolved, two color vibrational pump–probe spectroscopy.[1,2] In this method, the $v=0\rightarrow 1$ transition is pumped with an intense ps IR pulse. On a time scale short compared to the vibrational lifetime, a second IR probe, generally having a wide bandwidth, is passed through the sample and spectrally resolved. The $v=1\rightarrow 2$ transition appears as an absorption of the probe that is not present in the absence of the pump. This method has been successfully applied,[1,2] but it requires two ps IR pulses with different characteristics, i.e., wavelength and bandwidth.

An alternative approach is to perform a vibrational echo[3–6] using pulses having sufficiently wide bandwidth to establish a multilevel coherence among the $v=0$, 1, and 2 states.[7] The multilevel coherence results in a vibrational echo decay with beats. The beats occur at the frequency of the difference between the $v=0\rightarrow 1$ and $v=1\rightarrow 2$ transition energies, i.e., at the frequency of the vibrational anharmonic splitting. This is not a conventional quantum beat. In a quantum beat, a state is coupled by the radiation field directly to two other states that fall within the bandwidth of the pulse. In the vibrational echo anharmonic beat (VEB) experiment, the radiation field couples $v=0\rightarrow 1$ and then $v=1\rightarrow 2$. There is no direct coupling between $v=0\rightarrow 2$.

In addition to measuring the vibrational anharmonicity through the echo decay beat frequency, the echo decay provides the homogeneous dephasing time (homogeneous linewidth) of both the $v=0-1$ and $v=1-2$ transitions. The homogeneous linewidth provides information on the dynamical interactions of a vibration with its environment. Vibrational echo experiments on liquids,[4,5] glasses,[4,5] and proteins[6,8] have shown that vibrational spectra may be

[a]Permanent address: Department of Physics, Franklin and Marshall College, Lancaster, PA 17604.
[b]Present address: Department of Chemistry, University of Munich, 80290 Munich Germany.
[c]Present address: Department of Chemistry, University of Chicago, Chicago, IL 60637.
[d]Author to whom correspondence should be sent.

inhomogeneously broadened, even at room temperature. Therefore, vibrational echo experiments are necessary to extract the homogeneous linewidth from the observed spectroscopic line. The VEB experiment makes it possible to compare the homogeneous linewidths of the $v=0-1$ and $v=1-2$ transitions. At the polarization level for Lorentzian homogeneous lines, the echo decay is a bi-exponential squared with beats. One exponential corresponds to the decay of the $v=1-2$ coherence and the other exponential corresponds to the decay of the $v=0-1$ coherence. Therefore, the VEB experiment allows both the homogeneous linewidths and the vibrational anharmonicity to be experimental observables.

In this paper, VEB experiments on CO stretching modes of three molecules are presented: rhodiumdicarbonylacetylacetonate [$Rh(CO)_2acac$] and tungsten hexacarbonyl [$W(CO)_6$] in dibutylphthalate (DBP), and CO bound to the active site of a myoglobin protein in a 95:5 mixture of glycerol:water. The myoglobin protein is a mutant of wild type myoglobin in which the distal histidine (position 64) is replaced with a valine (H64V-CO).[6] The protein pocket around the CO in H64V is markedly different than either of the inorganic compounds. In the protein, the CO is bound to an octahedral Fe which has four bonds to a large aromatic macrocycle. The last bond of the Fe is to the proximal histidine (position 93).

The vibrational echo experiments on $Rh(CO)_2acac$ are the first for this molecule. Vibrational echo studies of $W(CO)_6$ in several liquid and glassy solvents have been reported,[3,5] including the first observation of vibrational echo anharmonic beats on $W(CO)_6$ in DBP.[7] Further, extensive vibrational echo studies and lifetime measurements of the $v=0-1$ transition have been presented previously for Mb–CO and H64V-CO.[6,8]

In the following, $Rh(CO)_2acac$ data is presented as a function of the excitation frequency. As the frequency is decreased, the beats become more pronounced. These results are compared to an approximate theoretical calculation, and the trends are found to be in accord. The $v=0-1$ and $v=1-2$ dephasing times and the anharmonicity are also obtained. For H64V-CO, the anharmonicity is much greater than in the two organometallic compounds. By tuning to lower frequencies than the $v=0\rightarrow1$ transition, beats are observed although the pulse bandwidth is insufficient to produce beats when centered on the $v=0\rightarrow1$ line. Again, the $v=0-1$ and $v=1-2$ dephasing times and the anharmonicity are obtained. These results are compared to prior measurements on $W(CO)_6$ in DBP.

II. THE NATURE OF THE EXPERIMENT AND PROCEDURES

In a vibrational echo experiment, two IR pulses, tuned to the frequency of the molecular vibration of interest, are crossed in the sample. The first pulse creates an ensemble of coherent superposition states that begin to dephase because of inhomogeneous broadening. A second pulse, delayed by time τ, is incident on the sample at an angle θ with respect to the first pulse and initiates rephasing of the inhomogeneous contributions to the vibrational spectral line. This rephasing results in a macroscopic polarization that is observed as an echo pulse at time 2τ. The echo emerges from the sample at an angle 2θ with respect to the first beam due to wave vector matching conditions. The integrated intensity of the echo pulse is measured as a function of τ.

For the case in which the laser bandwidth is narrow with respect to the vibrational anharmonicity, such that the vibrational coherence involves only the $v=0-1$ transition, the experiment is modeled well by a two level system. For a Lorentzian homogeneous lineshape with linewidth $\Gamma=1/\pi T_2$, the echo decays as

$$I(\tau)=I_0\ \exp(-4\gamma\tau), \tag{1}$$

where $\gamma=1/T_2$ for the $v=0-1$ transition. The homogeneous dephasing time has contributions from the pure dephasing time, T_2^*, and the vibrational lifetime, T_1,

$$\frac{1}{\pi T_2}=\frac{1}{\pi T_2^*}+\frac{1}{2\pi T_1}. \tag{2}$$

There can also be a contribution from orientational relaxation.[5] However, the experiments reported here were conducted in low temperature glassy solvents, so the contribution from orientational relaxation is negligible. The lifetime can be measured with a pump–probe experiment, and when combined with a vibrational echo measurement of T_2, the pure dephasing contribution to the homogeneous linewidth can be determined. For the systems studied here, the lifetime components of the homogeneous lines are only slightly temperature dependent. The pure dephasing components are more strongly temperature dependent.

When the laser bandwidth is similar to the anharmonicity, short pulse excitation will create a three level coherence involving the $v=0$, 1, and 2 vibrational levels. Previous theoretical work on a three level echo described an equally spaced system.[9] The derivation of the VEB signals for three level systems has a large contribution from experiments and theory studying coherent oscillations in semiconductor structures.[10,11] The echo signal can be described for an unequally spaced three-level system using a semiclassical diagrammatic perturbation theory treatment of the third-order nonlinear polarizability.[12,13] (See Appendix for details.) The three-level system is spaced by the frequencies ω_{01} and ω_{12}, where $\omega_{01}=\omega_{12}+\Delta$, and $\Delta\ll\omega_{01}$ and ω_{12}. Δ is the anharmonic vibrational energy splitting. The transition frequencies ω_{01} and ω_{12} lie within the bandwidth of the pulses. For such a system, three independent resonant pathways (diagrams) exist that result in rephasing and the generation of the echo pulse. (See Fig. 6 in the Appendix.) In addition to the two that describe a rephasing in a two level system,[13] a third diagram accounts for the possibility of rephasing the $v=1-2$ coherence. As discussed in the appendix, for a finite pulse bandwidth, where the E-field amplitude differs at ω_{01} and ω_{12}, the decay is given by[7]

$$I(\tau)=I(0)\exp(-2\gamma_{01}\tau)\{(E_{01}\cdot\mu_{01})^2\ \exp(-2\gamma_{01}\tau)+(E_{12}\cdot\mu_{12})^2\ \exp(-2\gamma_{12}\tau)-2(E_{01}\cdot\mu_{01})\times(E_{12}\cdot\mu_{12})\exp[-(\gamma_{01}+\gamma_{12})\tau]\cos(\Delta\tau+\phi)\}. \tag{3}$$

Here, E_{01} and E_{12} are amplitudes of the electric fields at the respective transitions and μ_{01} and μ_{12} are the respective dipole transition moments which are constant. γ_{01} and γ_{12} are the corresponding homogeneous dephasing decay constants, and Δ is the vibrational anharmonic splitting frequency (the beat frequency in the signal). $I(0)$ contains all the factors that determine the strength of the signal but are not involved in either the time dependent decays or the wavelength dependence of the beats. The dephasing rates for the two transitions, γ_{01} and γ_{12}, are phenomenological; no model has been assumed for the coupling of these modes to the bath. For the narrow bandwidth case ($E_{12}=0$), Eq. (1) is recovered. The phase factor in Eq. (3) does not arise from the derivation, i.e., $\phi=0$. As is standard in such derivations for which analytical results can be obtained, the pulse is taken to be a delta function in duration. Therefore, it has infinite bandwidth, and the E-field amplitude is independent of frequency. The derivation was modified by specifying different E-fields at the two transition frequencies. However, it has been shown that inclusion of the finite bandwidth of the pulses leads to a phase factor that need not be zero.[14] Therefore, the phase factor was included, and it was found to be an aid in fitting the data discussed below.

To compare Eq. (3) to data requires a convolution to account for the finite pulse duration. To extract an echo decay that is on the same time scale as the pulse duration requires full consideration of the three time ordered interactions of the radiation fields with the vibrations. In these experiments, the echo decays are long compared to the pulse durations, so this procedure is unnecessary. However, the beat frequency is comparable to the pulse duration. Therefore, in the data, the beats appear with much less depth of modulation than they would have in the absence of a finite instrument response. To account for this, Eq. (3) is convolved with the echo time dependence that would be observed for a sample with delta function response. This is defined as the instrument response function. For finite instrument responses, the data are fit by

$$S(\tau)=\mathfrak{T}^{-1}\{\mathfrak{T}[p(\sqrt{\tfrac{3}{2}}\tau)]x\mathfrak{T}[I(\tau)]\}, \tag{4}$$

where $\mathfrak{T}$ and $\mathfrak{T}^{-1}$ are Fourier transform and inverse Fourier transform, respectively. $I(t)$ is from Eq. (3), and $p(\tau)$ is the laser pulse envelope at the intensity level. In these experiments, the pulse envelope is an essentially transform limited Gaussian. The factor of $\sqrt{3/2}$ arises from the three interactions of the two Gaussian pulses used in the vibrational echo experiment. This procedure is the convolution of the sample response function with $\sqrt{3/2}$ times the Gaussian pulse envelope. There are two interactions with the second pulse, which gives rise to the pulse envelope squared. This is convolved with the first pulse. The net result is the square of the Gaussian pulse is convolved with the Gaussian pulse, yielding the $\sqrt{3/2}$ factor.

The vibrational echo experiments were performed using the Stanford Free Electron Laser (FEL). The FEL pulse train consists of a macropulse having a duration of $\sim$3 ms and repeating at 10 Hz. Within a macropulse is a series of micropulses repeating at 11.8 MHz. Each transform limited Gaussian micropulse has an energy of $\sim$0.5 μJ. The pulse duration was $\sim$1 ps (see below). The FEL frequency is actively stabilized to within 0.02% of the center frequency. Both the autocorrelation and the spectrum were monitored continuously during experiments.

The experimental apparatus is a slightly modified version of one reported previously.[6,8] Very briefly, the IR beam is split into two equal parts to become the two input pulses in the vibrational echo sequence. To reduce sample heating while retaining high peak power, single micropulses are selected from the macropulse at a reduced repetition rate using germanium acousto-optic modulators (AOM). One pulse is selected at $\sim$60 kHz, while the other is chopped to $\sim$30 kHz by a second AOM and sent through a motorized optical delay line. The chopping is performed to do background subtraction. The two beams are subsequently focused to $\sim$50 μm diameter spots in the sample using an off-axis paraboloidal mirror. The echo signal is subsequently focused onto an IR detector. The echo signal is acquired with a gated integrator and digitized by computer as the computer scans a stepper motor delay line.

The $W(CO)_6$ and H64V samples were prepared as reported previously.[6,7] The $Rh(CO)_2$acac sample was prepared as follows: $Rh(CO_2)$acac (Aldrich, 99%) was added to DBP (Aldrich, 99.9%) to a molarity of $\sim 1\times10^{-3}$. The sample was placed in a custom built copper housing between CaF_2 windows and an optical path of 400 μm. The samples were cooled using a He flow cryostat and the temperature was controlled to within 0.2 K.

III. RESULTS AND DISCUSSION

Figure 1(a) displays data taken on $Rh(CO)_2$acac in DBP at 3.4 K using a frequency of 2004.0 cm^{-1}. The center of the $v=0\rightarrow1$ transition is at 2010.1 cm^{-1}. So this data is taken with the frequency tuned somewhat to the red of the line center. The pulse bandwidth is 8 cm^{-1} FWHM, which corresponds to a 1.3 ps pulse duration. A fit to the data is also shown. The fit uses Eq. (3) convolved with a 1.6 ps FWHM instrument response. Figure 1(b) shows the same data but with a fit to Eq. (3) that holds the cosine term constant at one, i.e., the decay kinetics are the same but there are no beats in the fitting function. The inset in Fig. 1(b) are the residuals, which contain only the beats. Δ, the anharmonicity (the difference between the $v=0\rightarrow1$ and the $v=1\rightarrow2$ transition frequencies) can be obtained from the fit in Fig. 1(a) or it can be read off directly from the inset in Fig. 1(b). The results yield $\Delta=13.5\pm0.2$ cm^{-1}.

In the fit to Eq. (3), the fast component corresponds to the dephasing time of the $v=1-2$ vibrational coherence

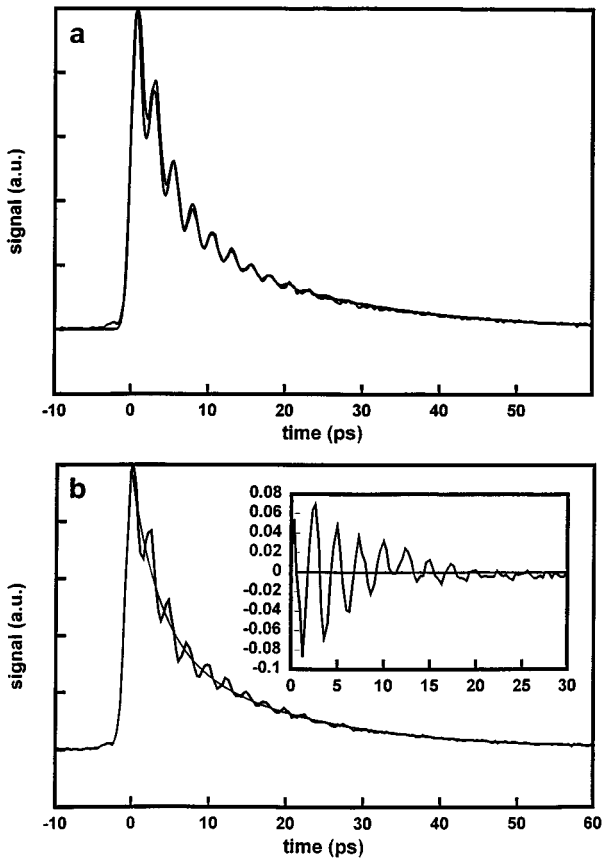

FIG. 1. (a) $Rh(CO)_2acac$ in DBP at 3.4 K and laser frequency of 2004.0 cm^{-1} and fit using Eqs. (3) and (4). The center of the $v=0\rightarrow1$ transition is at 2010.1 cm^{-1}. The pulse bandwidth is 8 cm^{-1} FWHM, which corresponds to a 1.3 ps pulse duration. The fit to the data uses Eq. (3) convolved with a 1.6 ps FWHM instrument response and yields T_2s of 15 and 92 ps for the $v=1\rightarrow2$ and $v=0\rightarrow1$ levels, respectively. (b) The same data but with a fit with Eq. (3) that holds the cos term constant at 1. The inset in (b) are the residuals. This is a method of displaying only the beats. Δ, the anharmonicity (the difference between the $v=0\rightarrow1$ and the $v=1\rightarrow2$ transition frequencies) can be obtained from the fit. The results yield $\Delta=13.5\pm0.2$ cm^{-1}.

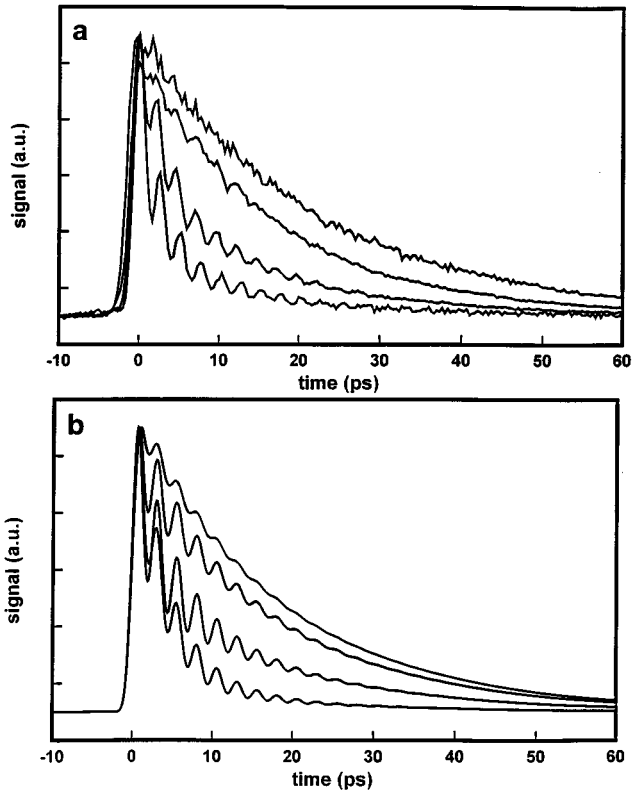

FIG. 2. (a) $Rh(CO)_2acac$ vibrational echo data taken at 3.4 K at laser frequencies, from top to bottom, 2020.2, 2012.1, 2004.0, and 1996.0 cm^{-1}. The center of the $v=0\rightarrow1$ transition is 2010.1 cm^{-1}. The dephasing times of the $v=1\rightarrow2$ and $v=0\rightarrow1$ transitions are 15 and 92 ps, respectively. (b) Calculated echo decays obtained using Eq. (3) for several ratios of the E-field amplitudes. These curves use lifetimes, beats frequencies, and phases determined from the $Rh(CO)_2acac$ data, and have been convolved with an 1.6 ps FWHM instrument response. Lines, from top to bottom in (b), have ratios of the E fields at the $v=0\rightarrow1$ and $v=1\rightarrow2$ transitions of 99.5/0.5, 95/5, 67/33, and 20/80, respectively. The calculation presented in (b) are qualitatively very similar to the data presented in (a).

$(T_2(12))$ and the slow component corresponds to the dephasing time of the $v=0-1$ vibrational coherence $(T_2(01))$. As can be seen from both Figs. 1(a) and 1(b), the fits to the data are quite good. The decay constants yield homogeneous dephasing times of $T_2(12)=15$ ps and $T_2(01)=92$ ps, respectively. In fitting the data, the phase factor ϕ in Eq. (3) was varied in addition to the other parameters. While the data can be fit with $\phi=0$, the fitting routine consistently returned values of $\phi\approx\pi/2$.

Equation (3) predicts that the magnitudes of the components of decay and the amplitude of the beats are related to the strengths of the E-fields at the two transition frequencies. For a finite bandwidth pulse, as the excitation frequency is moved from around the peak of the $v=0\rightarrow1$ transition to lower energies, the beats will become more pronounced, and the component of the decay corresponding to the relaxation of the $v=1-2$ coherence will become larger. Figure 2(a) displays $Rh(CO)_2acac$ vibrational echo data taken at 3.4 K at a variety of frequencies. The center of the $v=0\rightarrow1$ transition is 2010.1 cm^{-1}. The first data set is at 2020.2 cm^{-1}. In this data set, there are no apparent beats. These data can be fit with a single exponential, Eq. (1). At this laser frequency, there is little or no overlap of the pulse bandwidth with the $v=1\rightarrow2$ transition. The single exponential decay yields γ_{01} only. Tuning to lower energy, 2012.1 cm^{-1}, there are only very low amplitude beats, which are almost lost in the noise. However, the data cannot be fit well to a single exponential decay. To obtain a good fit, Eqs. (3) and (4) are needed. This frequency is still to the blue of the line center of the $v=0\rightarrow1$ transition, so the overlap of the pulse bandwidth with the $v=1\rightarrow2$ transition is small. The next data set, at 2004.0 cm^{-1}, definitely display beats. In this case, there is significant overlap of the pulse bandwidth with the $v=1\rightarrow2$ transition, and the beat amplitude and fast decay component magnitude increase markedly. Finally, the 1996.0 cm^{-1} data set shows significant beats as there is now extensive overlap of the excitation bandwidth with the $v=1\rightarrow2$ transition. All data sets indicate that the dephasing times of the $v=1-2$ and $v=0-1$ transitions are 15 and 92 ps, respectively. There is a clear phase shift in the data of

Fig. 2(a) that should be noticed. The phase shift may be explained by a full theoretical analysis of this problem using finite bandwidth pulses.[14]

Figure 2(b) shows calculated echo decays obtained using Eq. (3) for several ratios of the E-field amplitudes. These curves use dephasing times, beats frequencies, and phases determined from the $Rh(CO)_2$acac data, and have been convolved with an 1.6 ps FWHM instrument response. Lines A, B, C, and D in Fig. 2(b) have ratios of the $v=0\rightarrow1$ and $v=1\rightarrow2$ transition E-fields of 99.5/0.5, 95/5, 67/33, and 20/80, respectively. In the calculations, $\mu_{12}=\sqrt{2}\mu_{01}$, as is the case for a harmonic oscillator. As the quotient of the two E fields decreases, the amplitudes of the beats increase, and there is an increased short time decay of the signal because the contribution of the γ_{12} portion of the signal is increased. The magnitude of the beats in the simulation is also a function of the instrument response compared to the beat frequency. For all of the data presented in this paper, the instrument responses are in the 1 ps range. Since the beat frequencies are 2–5 ps, depending on the sample, the instrument response significantly decreases the observed magnitude of the beats. The calculation presented in Fig. 2(b) are qualitatively very similar to the data presented in Fig. 2(a). This demonstrates the basic validity of the description of the multilevel coherence and its frequency dependence. However, as discussed above and in detail in the Appendix, the analytical expression given in Eq. (3) was derived for a delta function duration pulse, but with the standard type of derivation modified to include different E fields at the two transition frequencies. A quantitative theoretical description of this problem cannot be obtained analytically because it will include a finite pulse duration with a finite bandwidth. This produces a complicated numerical problem that is under investigation.[14] As shown above, Eq. (3) provides a good description of the results. Because it is analytical, it is very useful in data fitting. It gives all parameters correctly except the depth of the beats.

Previously, an excitation frequency dependent study of vibrational beats on $W(CO)_6$ in DBT was reported.[7] These data display a frequency dependence which is substantially different from the data and calculations presented in Fig. 2. This difference probably arises because of the triple degeneracy of the T_{1u} CO transition of the $W(CO)_6$. The triple degeneracy is undoubtedly broken in the glassy environment. This will lead to many more pathways for the interaction of the radiation field with the system than are contained in the derivation of Eq. (3). The $Rh(CO)_2$acac CO stretching mode on which the experiments were performed is nondegenerate, and Eq. (3) provides a good description of the nondegenerate problem.

VEB measurements can be made on a large variety of systems. Figure 3 shows data taken on H64V in glycerol–water at 3.4 K with the laser tuned to 1957 cm^{-1}. The center of the $v=0\rightarrow1$ transition for this line is 1969 cm^{-1}. The excitation bandwidth for these data was ~16 cm^{-1} FWHM. When the echo decay is measured on line center, the data are a single exponential decay without beats. IR pump–probe experiments measured the $v=0\rightarrow1$ lifetime at this temperature as 35 ps.[15] Comparison of the line center echo decay and the pump–probe data demonstrate that at these low temperatures, the homogeneous dephasing time is approximately twice the lifetime $(2T_1)$, i.e., there is no significant pure dephasing. From the fit to the data, the decay constants, γ_{12} and γ_{01}, yield homogeneous dephasing times of $T_2(12)=20$ ps and $T_2(01)=65$ ps, respectively. The fit also gives the beat frequency. The inset in Fig. 3 displays only the beats, obtained in the same manner as described for Fig. 1(b). The data are modulated with a 1.3 ps beat which corresponds to an anharmonicity of 25.4 ± 0.2 cm^{-1}. This can be compared to the ~26 cm^{-1} anharmonicity reported for Mb-CO, which was measured using two color pump–probe experiments.[2] While H64V-CO has a shift in frequency and a 20% decrease in the rate of pure dephasing,[6] within experimental error, replacing the distal histidine with a valine does not change the CO vibrational anharmonicity.

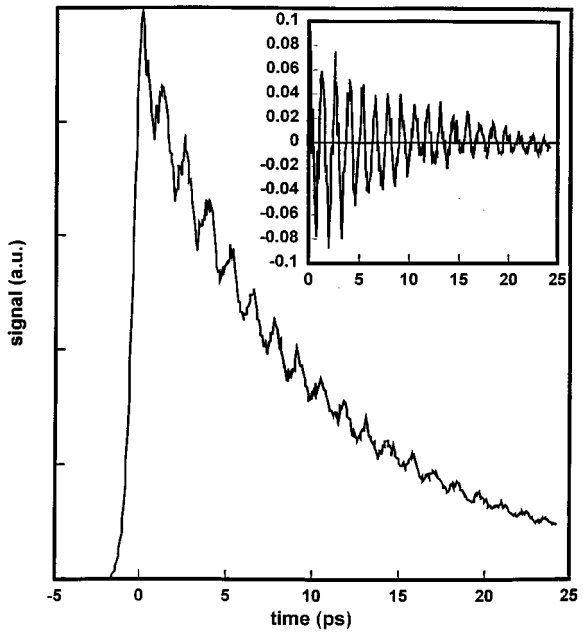

FIG. 3. Vibrational echo data on H64V in glycerol–water at 3.4 K with the laser tuned to 1957 cm^{-1}. The center of the $v=0\rightarrow1$ transition for this line is 1969 cm^{-1}. The excitation bandwidth was ~16 cm^{-1} FWHM. The dephasing times of the $v=1\rightarrow2$ and $v=0\rightarrow1$ transitions are 20 and 65 ps, respectively.

These data on H64V-CO show that it is possible to use the VEB method to obtain vibrational anharmonicities which are substantially larger than previously reported for $W(CO)_6$. Metal carbonyls with two or more equivalent carbonyls have very small anharmonicities. By using a pulse duration of 670 fs FWHM and tuning to lower frequency than the $v=0\rightarrow1$ line center, it was possible to measure the moderate anharmonicity of H64V-CO. Currently, it is not possible to produce significantly shorter pulses than 600 fs with the Stanford FEL. However, conventional laser/OPA systems can produce IR pulses which are substantially shorter. Therefore, using available technology, it should not be difficult to measure large anharmonicities of 100 cm^{-1} or more.

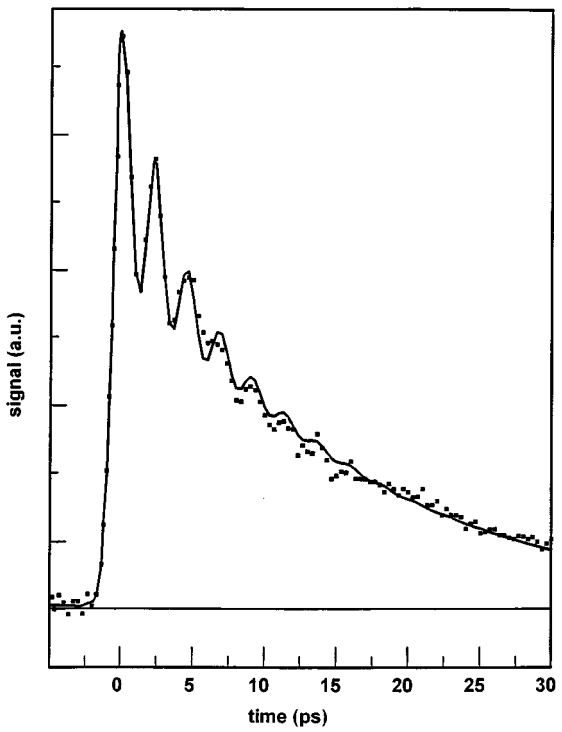

FIG. 4. Vibrational echo decay and fit $W(CO)_6$ in dibutylphthalate at 10 K and 1976.3 cm^{-1}. The beats are separated by 2.3 ps, corresponding to a vibrational anharmonic splitting of $\Delta = 14.7\ cm^{-1} \pm 0.3\ cm^{-1}$.

Figure 4 shows a vibrational echo decay for asymmetric CO stretching mode of $W(CO)_6$ in DBP at 10 K with the laser tuned to the center of the $v=0\rightarrow 1$ transition 1976.3 cm^{-1}, as well as a fit using Eq. (3).[7] The beats are separated by 2.3 ps, corresponding to a vibrational anharmonic splitting of $\Delta = 14.7\ cm^{-1} + \pm 0.3\ cm^{-1}$. This splitting is in accord with the value of $15\ cm^{-1} \pm 1\ cm^{-1}$ subsequently obtained by Heilweil and co-workers from observation of the $v=1\rightarrow 2$ and $v=2\rightarrow 3$ transitions of $W(CO)_6$ in hexane using two color pump–probe experiments.[1]

The experiments on $W(CO)_6$ were performed as a function of temperature.[7] From the fits to Eq. (3), the homogeneous dephasing times for the $v=0\rightarrow 1$ and $v=1\rightarrow 2$ transitions were obtained for temperatures between 10 and 150 K. These are displayed in Fig. 5. Detailed analysis of the temperature dependence of the $v=0-1$ dephasing demonstrates that by 10 K the homogeneous linewidth is dominated by the vibrational lifetime, i.e., $T_2 \approx 2T_1$.[5] From the fit to Eq. (3) of the data at 10 K and using results from Ref. 7 for the $v=0\rightarrow 1$ transition, the decay constants, γ_{12} and γ_{01}, yield homogeneous dephasing times of $T_2(12)=5.0$ ps and $T_2(01)=66$ ps, respectively. Above 10 K, the $v=0-1$ homogeneous linewidth increases as a power law, $T^{1.3}$.[5] However, the temperature dependence of the $v=1-2$ dephasing has a very different character. It is temperature independent up to ~ 90 K. This demonstrates that the $v=1-2$ dephasing is dominated by T_1 with $T_2 \approx 2T_1$ since a pure dephasing contribution to T_2 always displays a temperature dependence. Thus, at 10 K, both $T_2(01)$ and $T_2(12)$ are measures of the vibrational lifetimes of the two states.

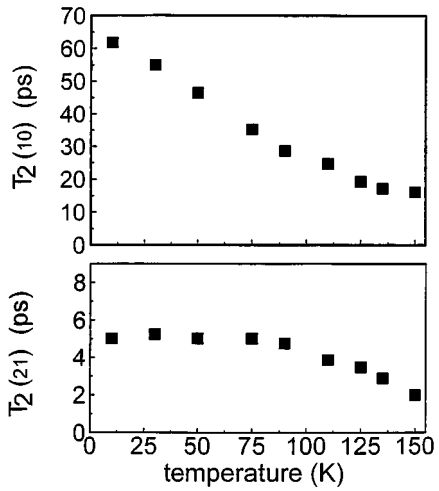

FIG. 5. Decay times $T_2(01)=1/\gamma_{01}$ and $T_2(12)=1/\gamma_{12}$ of $W(CO)_6$ in DBT for temperatures between 10 and 150 K obtained from fits to Eq. (3). The lack of temperature dependence of $T_2(12)$ at the lower temperatures shows that T_2 is lifetime limited.

The data for $W(CO)_6$ in DBP at 10 K demonstrates that $T_2 \approx 2T_1$ for both transitions. It is reasonable to assume that $T_2 \approx 2T_1$ for both transitions of $Rh(CO)_2$acac in DBP and for H64V-CO as well. These samples were studied at 3.4 K. It is known that $T_2 \approx 2T_1$ for the $v=0\rightarrow 1$ transitions in both samples at this temperature.[6,15] At these very low temperatures, the samples are in the low temperature limit. The thermal fluctuations of the heat bath are insufficient to cause significant pure dephasing. Even electronic transitions of large molecules in low temperature glasses have very slow pure dephasing times of ~ 1 ns.[16] These are only measurable because the electronic excited state lifetimes are long compared to the vibrational lifetimes discussed here. The coupling of vibrational transitions to the medium is much weaker than the coupling of electronic transitions as evidenced by much smaller gas to solvent shifts in transition frequencies and much slower pure dephasing at elevated temperatures. In addition, there is no fundamental reason why the pure dephasing of the $v=1-2$ transition should be different than the $v=0-1$ pure dephasing. For these reasons, we will take the T_2s of both transitions of all three samples to be lifetime limited at the lowest temperature.

The lifetimes, $T_1(1)$ and $T_1(2)$ of $v=1$ and $v=2$, respectively, and dephasing times $T_2(01)$ and $T_2(12)$ of the $v=0-1$ and $v=1-2$ transitions, respectively, are summarized in Table I. The approximate errors for $T_1(1)$ and $T_2(01)$ is 3%. The approximate error for $T_2(12)$ is 5%. Also reported in Table I are the ratios of lifetimes, $R_{T_1} = T_1(1)/T_1(2)$ and dephasing times, $R_{T_2} = T_2(01)/T_2(12)$.

The value of $T_1(1)$ is highly dependent on the choice of the solute–solvent systems studied. The lifetime of $W(CO)_6$ is solvent dependent. At room temperature, its lifetime in CCl_4 is ~ 700 ps, in $CHCl_3$ is ~ 340 ps, in 2-methylpentane is 150 ps. In the solvents $CHCl_3$ and 2-methylpentane, the lifetimes display an inverted temperature dependence,[17–19] i.e., the lifetimes become faster as the

TABLE I. Experimental results. Summary of the lifetimes, $T_1(1)$ and $T_1(2)$ of $v=1$ and $v=2$, respectively, and dephasing times $T_2(01)$ and $T_2(12)$ of the $v=0-1$ and $v=1-2$ transitions, respectively. The approximate errors of $T_1(1)$ and $T_2(01)$ is 3%. The approximate error for $T_2(12)$ is 5%. The approximate error for $T_1(2)$ is 10%. Also reported are the ratios of lifetimes, $R_{T_1}=T_1(1)/T_1(2)$ and dephasing times, $R_{T_2}=T_2(01)/T_2(12)$.

Sample	Anharmonicity	$T_2(01)$	$T_2(12)$	R_{T_2}	$T_1(1)$	$T_1(2)$	R_{T_1}
$W(CO)_6$	14.7 cm^{-1}	66 ps	5 ps	13	33 ps	3 ps	11
$Rh(CO)_2acac$	13.5 cm^{-1}	92 ps	15 ps	6	49 ps	9 ps	5
H64V-CO	25.4 cm^{-1}	65 ps	20 ps	3.3	35 ps	14 ps	2.5

temperature is decreased. In 2-methylpentane, the lifetime at 10 K is 100 ps. The change in lifetime with solvent shows that the solvent is intimately involved in the relaxation pathway. The initial CO vibration relaxes into a combination of solute and solvent modes plus a mode of the solvent continuum (solvent phonon) as necessary to conserve energy.[17–19] As the complexity of the solvent increases, more modes are available to provide a low-order pathway for the relaxation. In CCl_4, a fifth-order process is required that involves the annihilation of the initial excitation and the creation of three solute–solvent vibrational excitations and a phonon.[17–19] In $CHCl_3$, the addition of the CH bending mode at $\sim 1250\ cm^{-1}$ reduces the order of the process to fourth-order, and the lifetime is reduced.[17–19] 2-methylpentane has a wider variety of modes, and DBP an even wider variety. Presumably, these considerations are very similar for $Rh(CO)_2acac$.

However, H64V-CO, other Mb-COs, and a large variety of model heme-COs have been shown to relax in a different manner.[20–22] The relaxation is essentially solvent independent.[21,23,24] Relaxation occurs through deposition of the CO vibrational energy into the enormous density of states provided by the heme. The coupling has been shown to be via π-bond interactions. Back bonding from the metal–heme π electron system into the CO π^* antibonding molecular orbital couples the CO vibration directly to the vast number of heme vibrational states. An increase in the back bonding decreases the vibrational lifetime. Mb-CO has a lifetime of 16 ps. Replacing the distal histidine with a valine to form H64V-CO reduces the back bonding and slows the lifetime to 35 ps. Therefore, by selecting the particular form of Mb, it is possible to have a heme-CO system with a $v=1$ lifetime that is similar to the simpler metal carbonyls. This facilitates the comparison of the $v=1$ lifetimes and the $v=2$ lifetimes.

A striking feature of Table I is the trend in the ratios (R_{T_1}) of $T_1(1)$ to $T_1(2)$ for the three samples. In all cases, relaxation from $v=2$ is substantially faster than relaxation from $v=1$. In the most basic analysis, it would be expected that ratio $R_{T_1}=T_1(1)/T_1(2)$ would be 2.[25] This will occur if the density of bath states and the strength of coupling to the bath for the relaxation process are independent of the initial vibrational quantum number, v, and if no additional relaxation pathways become available for the higher v initial state. The action of a lowering operator contained in the vibrational relaxation coupling matrix element for a $v\rightarrow v-1$ relaxation brings out a factor of $\sqrt{v}$. The relaxation rate scales as the square of the matrix element. Therefore, when the initial state is 2, the $\sqrt{v}$ factor squared yields 2, and when the initial state is 1, the $\sqrt{v}$ factor squared yields 1, giving an R of 2. So from this consideration alone, the $v=1$ lifetime should be twice as long as the $v=2$ lifetime.

At low temperature, where there is no pure dephasing, T_2 is determined by $2T_1$. However, when looking at dephasing, if R_{T_1} is 2, the ratio, $R_{T_2}=T_2(01)/T_2(12)$ should be 3. The dephasing rate is the average of the rates of population decay out of the two levels involved. For dephasing of the $v=0-1$ transition,

$$\frac{1}{T_2(01)}=\frac{\gamma(1)+\gamma(0)}{2}=\frac{1}{2T_1(1)}, \tag{5}$$

where $\gamma(0)=1/T_1(0)$ and $\gamma(1)=1/T_1(1)$. Since the rate out of the ground state is 0, the common result for a $v=0-1$ vibrational echo of $T_2(01)=2T_1(1)$ is obtained. Rearranging Eq. (5) yields

$$\gamma(1)=\frac{2}{T_2(01)}. \tag{6}$$

The upper state dephasing is similar in that it is the average of the rates out of the two levels as given in Eq. (7)

$$\frac{1}{T_2(12)}=\frac{\gamma(1)+\gamma(2)}{2}. \tag{7}$$

The $v=2$ lifetimes displayed in Table I were calculated from measured values of the $v=1$ lifetimes $(\gamma(1)s)$ and the $v=1-2$ dephasing rates, using Eq. (7). The approximate error for these calculated lifetimes is 10%. As stated above, the minimum ratio of the upper and lower dephasing rates is 3. This follows from the simplification of Eq. (7) using the Landau–Teller model for which $\gamma(2)=2\gamma(1)$,

$$\frac{1}{T_2(12)}=\frac{\gamma(1)+\gamma(2)}{2}=\frac{3\gamma(1)}{2}. \tag{8}$$

Using the results of Eq. (6) in Eq. (8) yields

$$\frac{1}{T_2(12)}=\frac{3}{T_2(01)}. \tag{9}$$

Clearly, these factors of 2 and 3 alone do not account for the R_{T_1} and R_{T_2} listed in Table I, although they come very close for H64V-CO. The vibrational relaxation in the two metal carbonyls depends strongly on interactions with the solvent. The $v=1\rightarrow 2$ transition is shifted to lower energy

by $\sim 14\ \mathrm{cm}^{-1}$ for both molecules. The relaxation pathway almost certainly includes a phonon mode of the glassy solvent continuum. For a non-hydrogen bonding organic like DBP, the continuum extends to $\sim 200\ \mathrm{cm}^{-1}$.[26] Therefore, if the phonon mode is to the high energy side of the peak of the density of states, a $14\ \mathrm{cm}^{-1}$ shift to lower energy could result in an increase in the density of states, and therefore an increase in the vibrational relaxation rate for $v=2$. Also, an increase in the strength of coupling results from the participation of a different phonon. However, such a change is likely to only account for a portion of the R_{T_1} for $W(CO)_6$ and $Rh(CO)_2$acac. H64V-CO, which does not utilize the solvent in its relaxation would not have this effect.

A factor which may be the major contributor to the large R_{T_1} values of the simple metal carbonyls is the opening of a new relaxation pathway for relaxation from the $v=2$ state. The new pathway is direct relaxation from $v=2$ to $v=0$. The $v=2\rightarrow 0$ transitions for the systems studied have energies $\sim 3950\ \mathrm{cm}^{-1}$. It is possible for the numerous C–H transitions, which have energies in the $3300-2900\ \mathrm{cm}^{-1}$ range, to participate in the vibrational relaxation. If the $v=2\rightarrow 0$ relaxation is a low order path, perhaps not involving a phonon because of the large number of C–H modes covering a wide range of frequencies, it could substantially augment the rate of relaxation out of the $v=2$ level. The experiment measures the decay constant, γ_2, which is independent of the pathway for leaving the $v=2$ level. Relaxation from $v=2\rightarrow 0$ or from $v=2\rightarrow 1$ have the same effect on the decay of the coherence. While both $W(CO)_6$ and $Rh(CO)_2$acac have the $v=2\rightarrow 0$ opened, its influence on R_{T_1} will depend on the details of the coupling matrix elements and differences in the internal molecular modes that can participate in the relaxation. H64V-CO already has an enormous density of coupled states provided by the heme, and therefore, the availability of an additional pathway apparently makes less difference.

The ratio R_{T_1} in Table I can have at least three contributions: the factor of 2 which comes from the quantum number dependence through the lowering operator, a change in the phonon density of states, and the additional $v=2\rightarrow 0$ pathway. While all three molecules have similar $v=1$ lifetime, the experiments demonstrate that there can be a wide range of rates for decay out of the $v=2$ level. This range depends on the relative contribution of the three factors discussed above.

IV. CONCLUDING REMARKS

In this paper, we have investigated multilevel vibrational coherences observed in vibrational echo experiments in three systems, $Rh(CO)_2$acac in dibutylphthalate, H64V in glycerol–water, and $W(CO)_6$ in dibutylphthalate. The beats in the echo decay provide a direct measure of the vibrational anharmonicity. The observations in the three systems show that the VEB experiment can be of utility for measuring vibrational anharmonicities provided the coherence decay is sufficiently slow to permit observation of the beats. Equation (3) provides a good description of the observables. It permits extraction of the important physical parameters, i.e., the anharmonicity and the homogeneous linewidths of the $v=0-1$ transition and the $v=1-2$ transition. The frequency dependent $Rh(CO)_2$acac data demonstrates how the amplitudes of the beats, and, therefore, the extent of the multilevel coherence changes with the laser excitation frequency. Equation (3) can reproduce the general nature of the frequency dependence, but it does not provide a quantitative description because the derivation of the analytical expression does not include the finite duration of the excitation pulses.

At the very low temperatures of the experiments, the homogeneous dephasing times are determined by the vibrational lifetimes, $T_2 \approx 2T_1$. The three molecules studied have similar $v=1$ lifetimes, but the decays of the multilevel coherences observed in the vibrational echo experiments show that the $v=2$ lifetimes of all three molecules are significantly faster and that they vary from one molecule to another. Possible mechanisms for the decrease in the lifetimes and the variations were discussed.

To observe the VEB signal, it is necessary to have the transform limited bandwidth of the excitation pulses comparable to the anharmonic splitting. As demonstrated, the amplitude of the beats can be enhanced by tuning to lower frequency so the that the pulse bandwidth can more effectively overlap both the $v=0\rightarrow 1$ and $v=1\rightarrow 2$ transitions. However, it is important to emphasize that the shortest possible pulse duration (widest bandwidth) is not always desirable in a vibrational echo experiment. If the aim is to understand the dynamics of the a liquid, glass, or protein system by studying the pure dephasing of the $v=0-1$ transition, the multilevel coherence may interfere by turning a single exponential decay into a multiexponential decay with beats. At high temperatures, where the echo decay time can be comparable to the beat period, it can be difficult to extract the true echo decay. Therefore, it is desirable to use a pulse duration that is appropriate to obtain the information that is being sought.

ACKNOWLEDGMENTS

The authors would like to thank Professor Alan Schwettman and Professor Todd Smith, Physics Department, Stanford University, and their research groups at the Stanford Free Electron Laser Center whose efforts made these experiments possible. We would also like to thank Professor Dana D. Dlott and Professor Stephen G. Sligar, and Dr. Jeffrey R. Hill and Dr. Ellen Y. T. Chien for providing us with the H64V-CO sample used in these experiments. This research was supported by the Office of Naval Research, (N00014-94-1-1024), by the National Science Foundation, Division of Materials Research (DMR93-22504), and by the Office of Naval Research, (N00014-92-J-1227).

APPENDIX

We present a derivation of Eq. (3) in this Appendix. We use a standard Markovian model in the low temperature limit. This treatment is similar to that of Fourkas *et al.* where the signal was derived assuming $\omega_{12}=\omega_{01}$.[9]

There are three possible resonant quantum mechanical pathways that contribute to the vibrational echo signal (after $t=0$) when excitation bandwidth overlaps with three levels. These are shown in Figs. 6(a) and 6(b). Figure 6(a) is the ladder diagram representation of the resonant pathways. The solid arrows denote interactions on the ket of the density matrix, while dotted arrows denote interactions on the bra of the density matrix. The signal is indicated with the dashed arrows. The first two pathways are the standard ones for the vibrational echo involving two levels. The third pathway involves excited-state absorption, and hence, interferes with the first two.[9]

The general polarization is a sum of the individual response functions integrated over the excitation fields

$$P^{(3)}=\int_0^\infty d\omega G(\omega)\int_0^\infty dt_3\int_0^\infty dt_2\int_0^\infty dt_1\ \overline{E_1^*}\,\overline{E_2}\,\overline{E_3}\times\sum_i R_i(t_1,t_2,t_3), \tag{A1}$$

where t_1,t_2,t_3 are the times between each of the pulses in the vibrational echo sequence and R_i are the response functions. The distribution of transition frequencies, ω, is reflected by the inhomogeneous distribution function, $G(\omega)$. For delta function pulses

$$\overline{E_i}=|E_i|\,\delta(t-\tau_i)\exp(-i\omega t). \tag{A2}$$

The response functions are given by

$$R_1=R_2=\mu_{01}^4\exp(i\omega_{01}t_1-i\omega_{01}t_3)\exp(-\gamma_{01}t_1-\gamma_{01}t_3), \tag{A3}$$

$$R_3=-\mu_{01}^2\mu_{12}^2\exp(i\omega_{01}t_1-i\omega_{12}t_3)\exp(-\gamma_{01}t_1-\gamma_{12}t_3), \tag{A4}$$

where $I_{ij}(t)=\exp(-i\omega_{ij}t-\gamma_{ij}t)$ and $\mu_{ij}=|\langle i|\mu|j\rangle|$ and $\omega_{ij}=\omega_i-\omega_j$. Note that the complete derivation depends also on the t_2 time, which is the time between the second and third interactions. In the echo experiment, the second pulse provides both the second and third interactions so the time between them is zero for delta function pulses. Therefore, terms containing t_2 in Eq. (A3) and (A4) (and henceforth) have been dropped.

Since for a purely harmonic system, $\mu_{01}=\sqrt{2}\mu_{12}$, the third path will completely cancel the echo at $t=0$ and will cancel the echo signal at all time if $\omega_{12}=\omega_{01}$ and $\gamma_{01}=\gamma_{12}$.[9] However, in real systems, the oscillator is not harmonic, therefore $\omega_{12}\neq\omega_{01}$. As shown below, the beating in the data will arise from the difference between ω_{12} and ω_{01} and the decay of the beats will be the average of the γ_{01} and γ_{12} times.

To include inhomogeneous broadening, we take the distribution function to be a Gaussian centered at $\overset{\circ}{\omega}_{ij}$:

$$G(\omega_{ij})=\frac{1}{\sqrt{2\pi}\sigma}\exp\left(\frac{-(\omega_{ij}-\overset{\circ}{\omega}_{ij})^2}{2\sigma^2}\right)=G(\delta_{ij}), \tag{A5}$$

where δ_{ij} is the deviation from the center of the line. We will further assume that the distribution function for the ω_{01} transition is the same as the ω_{12} transition. Also, the inhomogeneous broadening is taken to be perfectly correlated in the two transitions. Further, all transitions for a given distribution have the same μ_{ij} and γ_{ij}.

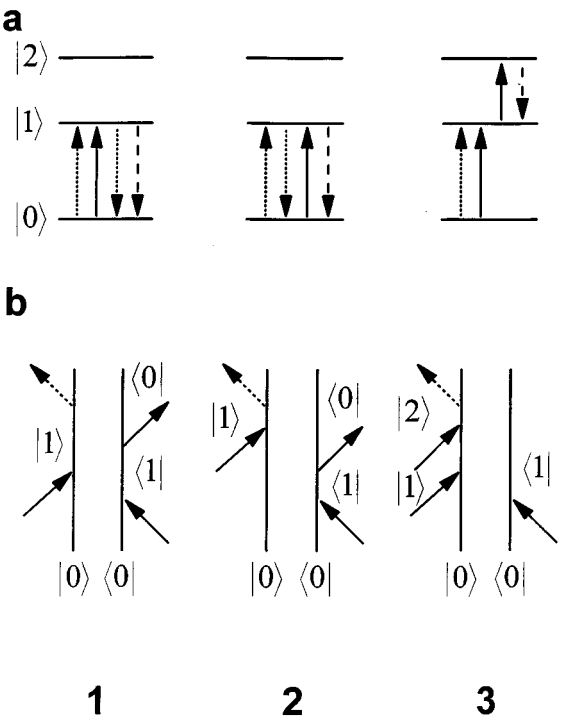

FIG. 6. (a) Latter diagram of the three pulse sequences in a VEB experiment. The first two diagrams are the two-level vibrational echo diagrams. The solid arrows denote interactions on the ket of the density matrix, while dotted arrows denote interactions on the bra of the density matrix. The signal is indicated with the dashed arrows. (b) Another representation of the three pulse sequences of in the VEB experiment. Time is taken to increase moving up the parallel set of lines.

In the delta function pulse limit, the polarization is given by the response function

$$P^{(3)}(t_3,t_1)=\int_0^\infty G(\delta_{ij})\left[\sum_i R_i(t_i,t_3,\delta)\right]|E_1^*||E_2||E_3|d\delta_{ij}, \tag{A6}$$

substituting $\omega_{ij}=\omega_{ij}^0+\delta_{ij}$ yields

$$R_1=R_2=\mu_{01}^4\exp[i\omega_{01}(t_1-t_3)]\times\exp[-\gamma_{01}(t_1+t_3)]\exp[i\delta(t_1-t_3)], \tag{A7}$$

$$R_3=-\mu_{01}^2\mu_{12}^2\exp(i\omega_{01}t_1-i\omega_{12}t_3-\gamma_{01}t_1-\gamma_{12}t_3)\times\exp[i\delta(t_1-t_3)]. \tag{A8}$$

Substituting Eqs. (A7) and (A8) into Eq. (A6) yields the third-order polarization as

$$P^{(3)}(t_3,t_1)=|E_1^*||E_2||E_3|\exp\left(\frac{-(t_3-t_1)^2\sigma^2}{2}\right)\times\{2\mu_{01}^4\exp[i\omega_{01}(t_1-t_3)]\times\exp[-\gamma_{01}(t_1+t_3)]-\mu_{01}^2\mu_{12}^2\times\exp(i\omega_{01}t_1-i\omega_{12}t_3-\gamma_{01}t_1-\gamma_{12}t_3)\}. \tag{A9}$$

This shows the echo characteristic of being sharply peaked at $t_1=t_3$, if the distribution function is very broad.

The observed integrated signal is

$$S(t)=\int_{-\infty}^{+\infty} dt_3 |P(t_1-t_3)|^2. \tag{A10}$$

Defining the intensity as the square of the absolute value of the E-field and substituting Eq. (A9) into Eq. (A10) yields

$$\begin{aligned} S(t)=I^3[&4\mu_{01}^8 \exp(-4\gamma_{01}t)+\mu_{01}^4\mu_{12}^4 \exp(-2\gamma_{01}t \\ &-2\gamma_{12}t)-2\mu_{01}^6\mu_{12}^2 \exp(-3\gamma_{01}t-\gamma_{12}t) \\ &\times\{\exp[i(\omega_{01}-\omega_{12})t]+\exp[-i(\omega_{01}-\omega_{12})t]\}, \end{aligned} \tag{A11}$$

which simplifies to

$$\begin{aligned} S(t)=I^3[&\exp(-2\gamma_{01}t)][\mu_{01}^8 \exp(-2\gamma_{01}t) \\ &+\mu_{01}^4\mu_{12}^4 \exp(-2\gamma_{12}t)+\mu_{01}^6\mu_{12}^2 \\ &\times\exp(-\gamma_{01}t-\gamma_{12}t)\cos(\Delta t)]. \end{aligned} \tag{A12}$$

This derivation assumed delta function pulses with infinite bandwidth. Therefore, the E fields have no frequency dependence. There is no frequency dependence in Eq. (A12). In particular, the depth of the modulation occurring at frequency, Δ, is independent of the laser frequency. The depth depends only on the values of the μ_{01} and μ_{12}, which are constants. This is in contradiction to the data in Fig. 2(a). The use of a delta function duration pulse makes it possible to obtain an analytical expression. In the experiments, the laser pulses have finite durations and, therefore, finite bandwidths. The finite bandwidth results in different driving E fields, E_{01} and E_{12}, at the two transition frequencies. When the frequency is changed, the values of E_{01} and E_{12} change, giving rise to the frequency dependence displayed in Fig. 2(a). For a two level system, the coherence is produced by the coupling of the radiation field to the transition dipole as $(E\cdot\mu)$. To include the effect of finite bandwidth pulses and yet preserve the analytical expression, we associate E_{ij} with μ_{ij} where appropriate. This results in Eq. (A13),

$$\begin{aligned} S(t)=&(E_{01}\cdot\mu_{01})^4[\exp(-2\Gamma_{01}t)][4(E_{01}\cdot\mu_{01})^2\mu_{01}^2 \\ &\times\exp(-2\Gamma_{01}t)+(E_{12}\cdot\mu_{12})^2\mu_{12}^2 \exp(-2\Gamma_{12}t) \\ &-4(E_{01}\cdot\mu_{01})^2(E_{12}\cdot\mu_{12})^2\mu_{01}\mu_{12} \exp(-\Gamma_{01}t \\ &-\Gamma_{12}t)\cos(\Delta t)]. \end{aligned} \tag{A13}$$

As can be seen from Figs. 6(a) and 6(b), all three pathways have the first two interactions involving only the $v=0-1$ transition. These interactions give rise to the first term. The extra factors of μ^2 not multiplied by E^2 give rise to the signal.

[1] S. M. Arrivo, T. P. Dougherty, W. T. Grubbs, and E. J. Heilweil, Chem. Phys. Lett. **235**, 247 (1995).
[2] J. C. Owrutsky, M. Li, B. Locke, and R. M. Hochstrasser, J. Phys. Chem. **99**, 4842 (1995).
[3] D. Zimdars, A. Tokmakoff, S. Chen, S. R. Greenfield, and M. D. Fayer, Phys. Rev. Lett. **70**, 2718 (1993).
[4] A. Tokmakoff, D. Zimdars, R. S. Urdahl, R. S. Francis, A. S. Kwok, and M. D. Fayer, J. Phys. Chem. **99**, 13310 (1995).
[5] A. Tokmakoff and M. D. Fayer, J. Chem. Phys. **102**, 2810 (1995).
[6] K. D. Rector, C. W. Rella, A. S. Kwok, J. R. Hill, S. G. Sligar, E. Y. T. Chien, D. D. Dlott, and M. D. Fayer, J. Phys. Chem. B **101**, 1468 (1997).
[7] A. Tokmakoff, A. S. Kwok, R. S. Urdahl, R. S. Francis, and M. D. Fayer, Chem. Phys. Lett. **234**, 289 (1995).
[8] C. W. Rella, K. Rector, A. Kwok, J. R. Hill, H. A. Schwettman, D. D. Dlott, and M. D. Fayer, J. Phys. Chem. **100**, 15620 (1996).
[9] J. T. Fourkas, H. Kawashima, and K. A. Nelson, J. Chem. Phys. **103**, 4393 (1995).
[10] X. Zhu, M. S. Hybertsen, P. B. Littlewood, and M. C. Nuss, Phys. Rev. B **50**, 11915 (1994).
[11] S. T. Cundiff, Phys. Rev. A **49**, 3114 (1994).
[12] S. Mukamel and R. F. Loring, J. Opt. Soc. B **3**, 595 (1986).
[13] Y. J. Yan and S. Mukamel, J. Chem. Phys. **94**, 179 (1991).
[14] J. Fourkas (private communication).
[15] K. D. Rector and M. D. Fayer (unpublished).
[16] L. R. Narasimhan, K. A. Littau, D. W. Pack, Y. S. Bai, A. Elschner, and M. D. Fayer, Chem. Rev. **90**, 439 (1990).
[17] A. Tokmakoff, B. Sauter, and M. D. Fayer, J. Chem. Phys. **100**, 9035 (1994).
[18] V. M. Kenkre, A. Tokmakoff, and M. D. Fayer, J. Chem. Phys. **101**, 10618 (1994).
[19] P. Moore, A. Tokmakoff, T. Keyes, and M. D. Fayer, J. Chem. Phys. **103**, 3325 (1995).
[20] J. R. Hill, D. D. Dlott, M. D. Fayer, C. W. Rella, M. M. Rosenblatt, K. S. Suslick, and C. J. Ziegler, J. Phys. Chem. **100**, 218 (1996).
[21] J. R. Hill, M. M. Rosenblatt, C. J. Ziegler, K. S. Suslick, D. D. Dlott, C. W. Rella, and M. D. Fayer, J. Phys. Chem. **100**, 18023 (1996).
[22] D. D. Dlott, M. D. Fayer, J. R. Hill, C. W. Rella, K. S. Suslick, and C. J. Ziegler, J. Am. Chem. Soc. **118**, 7853 (1996).
[23] A. Ansari, J. Beredzen, D. Braunstein, B. R. Cowen, H. Frauenfelder, M. K. Hong, I. E. T. Iben, J. B. Johnson, P. Ormos, T. Sauke, R. Schroll, A. Schulte, P. J. Steinback, J. Vittitow, and R. D. Young, Biophys. Chem. **26**, 337 (1987).
[24] D. Ivanov, J. T. Sage, M. Keim, J. R. Powell, S. A. Asher, and P. M. Champion, J. Am. Chem. Soc. **116**, 4139 (1994).
[25] L. Landau and E. Teller, Phys. Z. Sov. **10**, 34 (1936).
[26] Y. J. Chang and E. W. Castner, Jr., J. Phys. Chem. **100**, 3330 (1996).